

Image Restoration

Introduction to Signal and Image Processing

Prof. Dr. Philippe Cattin

MIAC, University of Basel

April 19th/26th, 2016

Contents

• Abstract	2
• 1 Image Degradation & Restoration Model	
◦ Image Degradation & Restoration Model	4
◦ Image Degradation & Restoration Model (2)	5
• 2 Noise Models	
◦ Noise Models	7
◦ Gaussian Noise	8
◦ Rayleigh Noise	9
◦ Erlang Noise	10
◦ Exponential Noise	11
◦ Uniform Noise	12
◦ Impulse (Salt-and-Pepper) Noise	13
◦ Noise Models	14
◦ Visual Comparison of Different Noise Sources	15
◦ Periodic Noise	16
◦ Estimation of Noise Parameters (1)	17
◦ Estimation of Periodic Noise Parameters	18
• 3 Restoration in the Precense of Noise Only	
◦ Restoration in the Precense of Noise Only	20
• 4 Periodic Noise Reduction by Frequency Domain Filtering	
◦ 4.1 Bandreject Filter	
■ Bandreject Filter	23
■ Bandreject Filter Example	24
◦ 4.2 Bandpass Filter	

▪ Bandpass Filter	26
▪ Bandpass Filter Example	27
◦ 4.3 Notch Filter	
▪ Notch Filter	29
▪ Notch Filter (2)	30
▪ Ideal Notch Filter $D_0=16$ Example	31
▪ Butterworth Notch Filter $D_0=64$ Example	32
▪ Gaussian Notch Filter $D_0=64$ Example	33
▪ General Notch Filter Example	34
◦ 4.4 Optimum Notch Filtering	
▪ Optimum Notch Filtering	36
▪ Optimum Notch Filtering Principle	37
▪ Optimum Notch Filter Example	38
▪ Optimum Notch Filter Example with Pixel Increments	39
▪ Optimum Notch Filter Example with Pixel Increments (2)	40
• 5 Estimating the Degradation Function	
◦ Estimating the Degradation Function	42
◦ Estimating the Degradation Function (2)	43
◦ Estimating by Image Observation	44
◦ Estimating by Experimentation	45
◦ Estimating by Mathematical Modelling	46
◦ Illustration of the Atmospheric Turbulence Model	47
• 6 Inverse Filtering	
◦ 6.1 Direct Inverse Filtering	
▪ Direct Inverse Filtering	50
▪ Two Practical Approaches for Inverse Filtering	51

▪ Artificial Inverse Filtering Example	52
▪ Artificial Inverse Filtering Example (2)	53
▪ Inverse Filtering Example (2)	54
◦ 6.2 Wiener Filtering	
▪ Wiener Filtering	56
▪ Wiener Filtering (2)	57
▪ Parametric Wiener Filter	58
▪ Artificial Wiener Filtering Example	59
▪ Wiener Filtering Example with Little Noise	60
▪ Wiener Filtering Example with Medium Noise	61
▪ Wiener Filtering Example with Heavy Noise	62
▪ Comparison Param. Wiener vs. Wiener Filtering	63
▪ Drawback of the Wiener Filter	64
◦ 6.3 Geometric Mean Filter	
▪ Geometric Mean Filter	66
◦ 6.4 Constrained Least Squares Filtering	
▪ Constrained Least Squares (Regularised) Filtering	68
▪ Constrained Least Squares Filtering (2)	69
▪ Constrained Least Squares Filtering (3)	70
▪ Optimal Selection for Gamma	71
▪ Artificial Constrained Least Squares Filter Example	72
▪ Constrained Least Squares Filter Example	73

Abstract (2)

As in image enhancement the goal of restoration is to improve an image for further processing. In contrast to image enhancement that was subjective and largely based on heuristics, restoration attempts to reconstruct or recover an image that has been distorted by a known degradation phenomenon. Restoration techniques thus try to model the degradation process and apply the inverse process in order to reconstruct the original image.

Image Degradation & Restoration Model

Image Degradation & Restoration Model (4)

The degradation process is generally modelled as a degradation function H and the additive noise term $\eta(x, y)$ together they yield $g(x, y)$.

Given $g(x, y)$, some knowledge about H , and $\eta(x, y)$ it is the objective of restoration to estimate $\hat{f}(x, y)$. Of course this estimate should be *as close as possible* to $f(x, y)$.

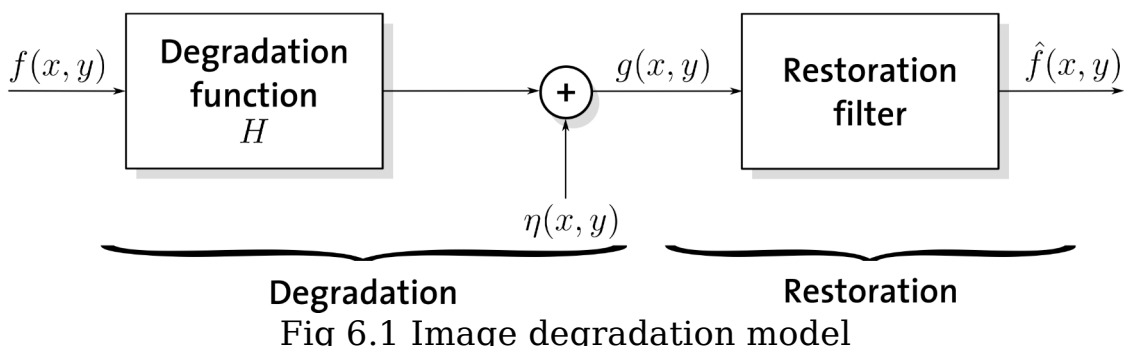


Image Degradation & Restoration Model (2) (5)

If the degradation function H is a linear, shift-invariant process, then the degraded image is given in the spatial domain by

$$g(x, y) = h(x, y) * f(x, y) + \eta(x, y) \quad (6.1)$$

where $h(x, y)$ is the spatial representation of the degradation function, and $*$ indicates convolution.

As we know from the Convolution Theorem this can be rewritten in the frequency domain

$$G(u, v) = H(u, v)F(u, v) + N(u, v) \quad (6.2)$$

where the capital letters are the Fourier transforms of the respective function in Eq [6.1](#).

Noise Models

Noise Models (7)

The principle *sources of noise* in digital images arise during image *acquisition* and/or *transmission*.

The performance of imaging sensors are affected by a variety of factors during acquisition, such as

- Environmental conditions during the acquisition
- Light levels (low light conditions require high gain amplification)
- Sensor temperature (higher temp implies more amplification noise)

Images can also be corrupted during transmission due to interference in the channel for example

- Lightning or other
- Atmospheric disturbances

Depending on the specific *noise* source, a *different model* must be selected that accurately *reproduces* the *spatial characteristics* of the noise.

Gaussian Noise (8)

Because of its mathematical tractability in both the spatial and frequency domain, Gaussian noise models (aka normal distribution) are used frequently in practice.

The PDF (Probability density function) of a Gaussian random variable z is given by

$$p_G(z) = \frac{1}{\sqrt{2\pi}\sigma} e^{-(z-\mu)^2/(2\sigma^2)} \quad (6.3)$$

where z represents the grey level, μ the mean value and σ the standard deviation.

The application of the Gaussian model is so convenient that it is often used in situations in which they are marginally applicable at best.

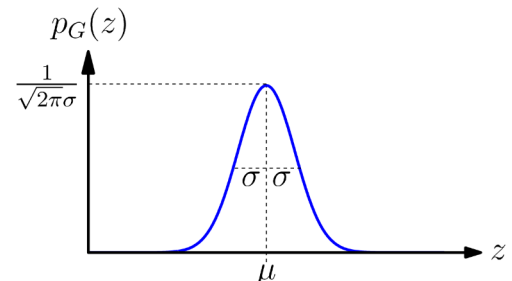


Fig 6.2: Gaussian probability density function $p_G(z)$

Rayleigh Noise (9)

The PDF of Rayleigh noise is defined by

$$p_R(z) = \begin{cases} \frac{2}{b}(z - a)e^{-\frac{(z-a)^2}{b}} & \text{for } z \geq a \\ 0 & \text{for } z < a \end{cases} \quad (6.4)$$

the mean and variance are given by

$$\mu = a + \sqrt{\pi b / 4} \quad (6.5)$$

$$\sigma^2 = \frac{b(4 - \pi)}{4}$$

As the shape of the Rayleigh density function is skewed it is useful for approximating skewed histograms.

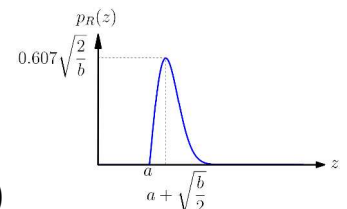


Fig 6.3: Rayleigh probability density function $p_R(z)$

Erlang Noise (10)

The PDF of the Erlang noise is given by

$$p_E(z) = \begin{cases} \frac{a^b z^{b-1}}{(b-1)!} e^{-az} & \text{for } z \geq 0 \\ 0 & \text{for } z < 0 \end{cases} \quad (6.6)$$

where $a > 0$, b is a positive integer. The mean and variance are then given by

$$\mu = \frac{b}{a} \quad (6.7)$$

$$\sigma^2 = \frac{b}{a^2}$$

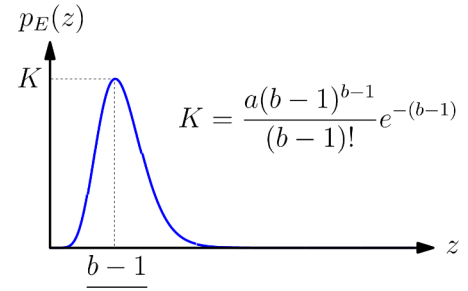


Fig 6.4: Erlang probability density function $p_E(z)$

Exponential Noise (11)

The PDF of the exponential noise is given by

$$p_{exp}(z) = \begin{cases} ae^{-az} & \text{for } z \geq 0 \\ 0 & \text{for } z < 0 \end{cases} \quad (6.8)$$

where $a > 0$. The mean and variance of the density function are

$$\mu = \frac{1}{a} \quad (6.9)$$

$$\sigma^2 = \frac{1}{a^2}$$

The exponential noise model is a special case of the Erlang noise model with $b = 1$.



Fig 6.5: Probability density function $p_{exp}(z)$ of exponential noise

Uniform Noise (12)

The PDF of the uniform noise is given by

$$p_U(z) = \begin{cases} \frac{1}{b-a} & \text{for } a \leq z \leq b \\ 0 & \text{for otherwise} \end{cases} \quad (6.10)$$

The mean and variance of the density function are given by

$$\mu = \frac{a+b}{2} \quad (6.11)$$

$$\sigma^2 = \frac{(b-a)^2}{12}$$

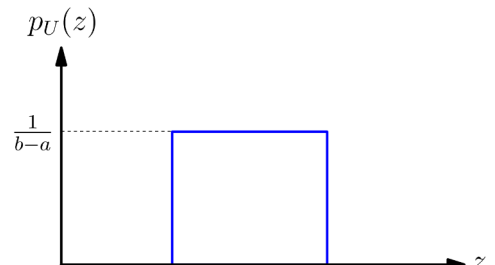


Fig 6.6: Probability density function $p_U(z)$ of uniform noise

Impulse (Salt-and-Pepper) Noise (13)

The PDF of bipolar impulse noise model is given by

$$p_I(z) = \begin{cases} P_a & \text{for } z = a \\ P_b & \text{for } z = b \\ 0 & \text{otherwise} \end{cases} \quad (6.12)$$



Fig 6.7: Probability density function $p_I(z)$ of the bipolar impulse noise model

If $b > a$, grey-level b appears as a light dot (salt) in the image. Conversely, a will appear as dark dot (pepper). If either P_a, P_b is zero, the PDF is called unipolar.

Because *impulse corruption* is generally *large* compared to the signal strength, the assumption is usually that a and b are digitised as *saturated values* thus *black* (pepper) and *white* (salt).

Noise Models (14)

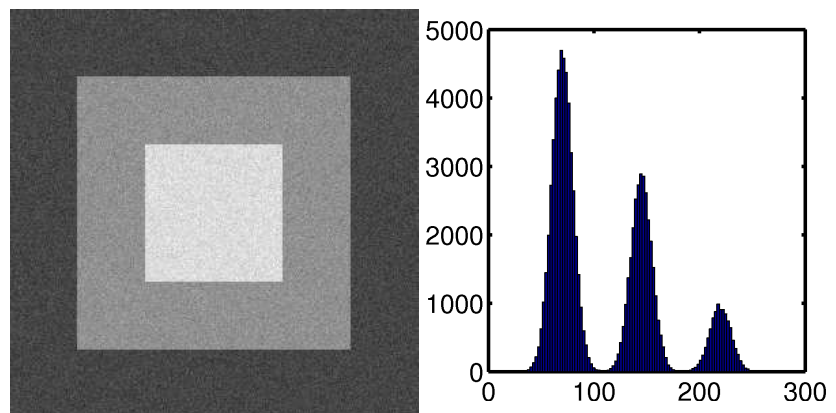
The presented noise models provide a useful tool for approximating a broad range of noise corruption situations found in practice. For example:

- Gaussian noise: arises in images due to *sensor noise* caused by *poor illumination* and/or *high temperature*, and *electronic circuit noise*
- The Rayleigh noise model is used to characterise noise phenomena in *range images*
- Exponential and Erlang noise models find their application in *Laser imaging*
- Impulse noise takes place in situations where *high transients* (faulty switching) occurs

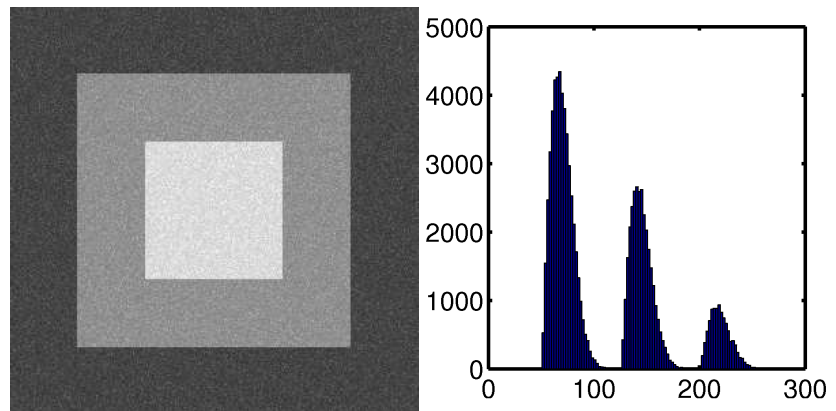
Visual Comparison of (15) Different Noise Sources

Although the corresponding histograms show close resemblance to the PDF of the respective noise model, it is virtually impossible to select the type of noise causing the degradation from the image alone.

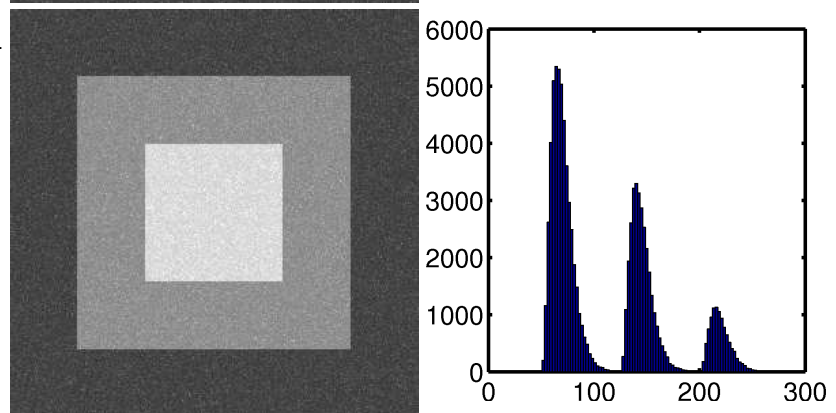
Gaussian noise
model



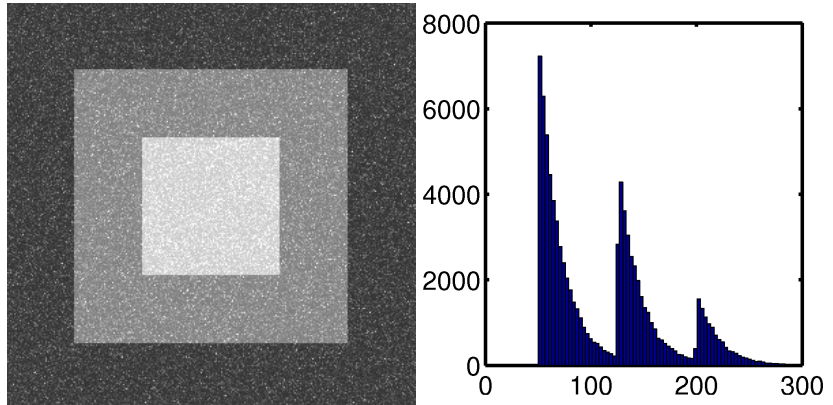
Rayleigh noise
model



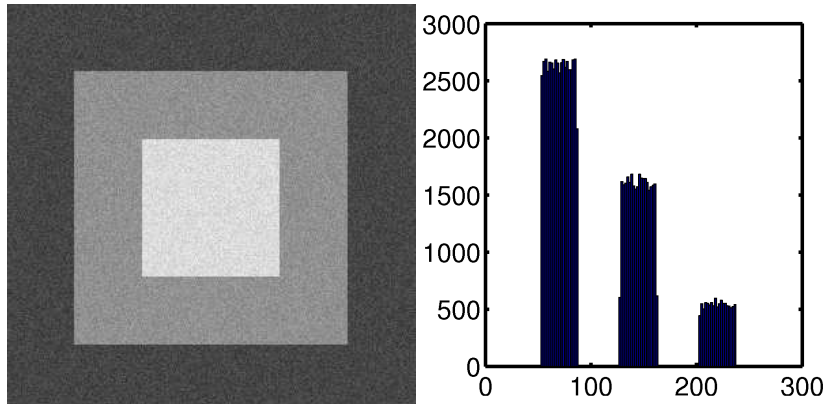
Erlang noise model



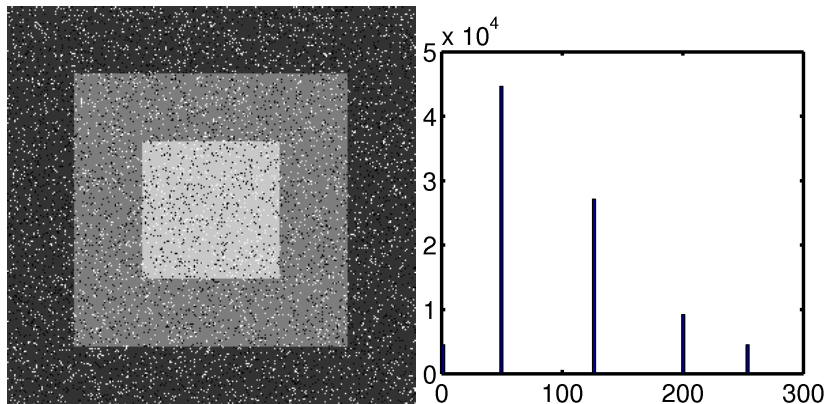
Exponential noise model



Uniform noise model



Impulse noise model
(Salt & Pepper)



Periodic Noise (16)

Periodic noise typically arises from electrical or electromechanical interference during image acquisition and is spatial dependent.



Fig 6.8: Periodic noise on a satellite image of Pompeii

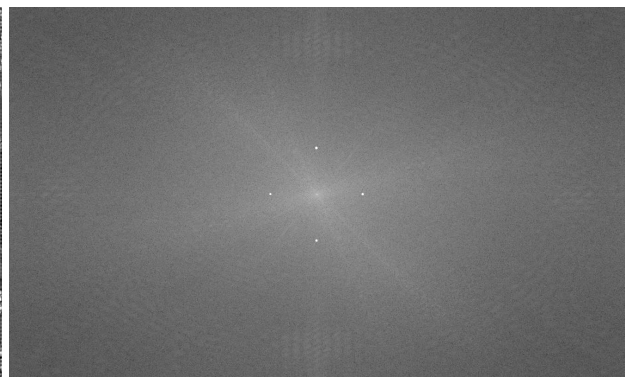


Fig 6.9: Spectrum of the Pompeii image with periodic noise (peaks of the periodic noise visually enhanced)

Estimation of Noise Parameters (1) (17)

In rare cases the *parameters* of noise PDFs may be known from *sensor specifications*, but it is *often necessary* to *estimate* them for a particular imaging arrangement.

If the *imaging system* is *available*, one simple way to study noise characteristics would be to *capture* multiple images of homogeneous environments, such as solid *grey cards*.

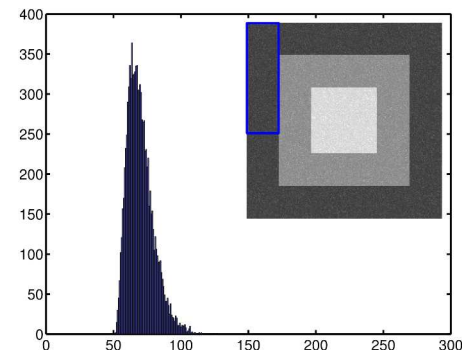


Fig 6.10: Sample histogram of a small patch of Erlang noise

In many cases the noise parameters have to be *estimated* from already *captured images*. The simplest way is to estimate the mean and variance of the grey levels from *small patches* of reasonably *constant grey level*.

Estimation of Periodic Noise Parameters (18)

The *parameters* of periodic noise are typically *estimated by inspection* of the *Fourier spectrum*. The frequency spikes can often be detected by visual analysis.

Automatic analysis is possible if the noise spikes are either exceptionally pronounced or a priori knowledge about their location is known.



Fig. 6.11:

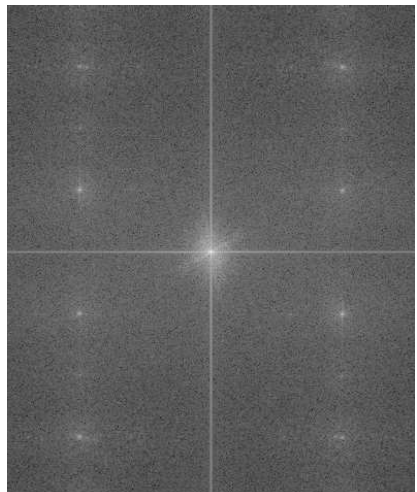


Fig. 6.12:

Restoration in the Precense of Noise Only

Restoration in the Precense of Noise Only (20)

When noise is the only image degradation present in an image, thus $H(u, v) = 1$, Eqs 6.1 & 6.2 become

$$g(x, y) = f(x, y) + \eta(x, y) \quad (6.13)$$

and

$$G(u, v) = F(u, v) + N(u, v) \quad (6.14)$$

In case of *periodic noise*, it is usually *possible to estimate* $N(u, v)$ from the spectrum of $G(u, v)$ and subtract it to obtain an estimate of the original image $f(x, y)$.

But *estimating the noise terms* $\eta(x, y)$ is *unreasonable*, so subtracting them from $g(x, y)$ is impossible. *Spatial filtering* is the *method of choice* in situations when only additive noise is present.

Periodic Noise Reduction by Frequency Domain Filtering

Bandreject Filter

Bandreject Filter (23)

Bandreject filters remove or attenuate a band of frequencies around the origin in the Fourier domain.

Ideal Bandreject Filter

$$H(u, v) = \begin{cases} 1 & \text{if } D(u, v) < D_0 - \frac{W}{2} \\ 0 & \text{otherwise} \\ 1 & \text{if } D(u, v) > D_0 + \frac{W}{2} \end{cases} \quad (6.15)$$

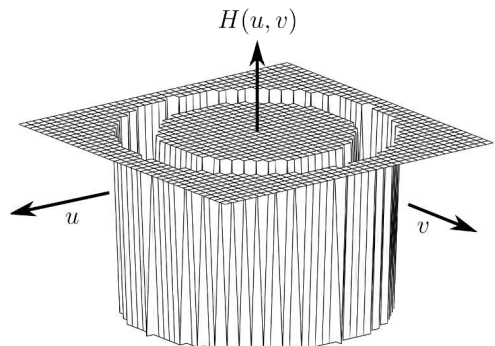


Fig 6.13: Ideal bandreject filter

Butterworth Bandreject Filter

$$H(u, v) = \frac{1}{1 + \left[\frac{D(u, v)W}{D^2(u, v) - D_0^2} \right]^{2n}} \quad (6.16)$$

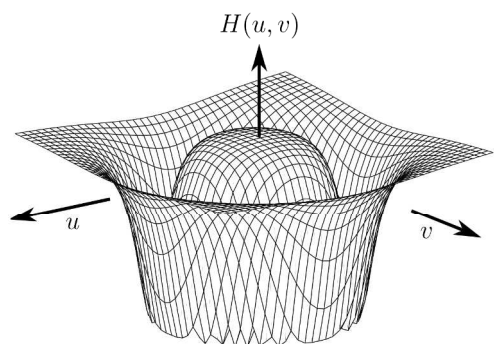


Fig 6.14: Butterworth bandreject filter

Gaussian Bandreject Filter

$$H(u, v) = 1 - e^{-\frac{1}{2} \left[\frac{D^2(u, v) - D_0^2}{D(u, v)W} \right]^2} \quad (6.17)$$

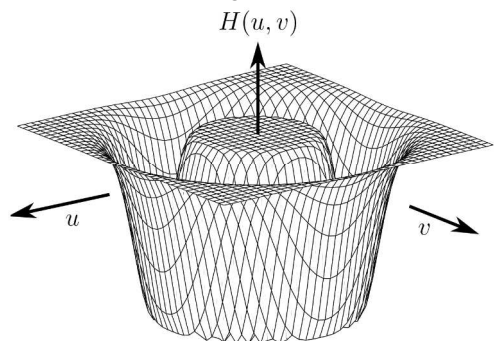


Fig 6.15: Gaussian bandreject filter

Bandreject Filter Example (24)



Fig 6.16: Aerial image of Pompeii with periodic noise



Fig 6.17: Ideal bandreject filter
 $D_0 = 100, W = 6$



Fig 6.18: Butterworth bandreject filter
 $D_0 = 100, W = 6$



Fig 6.19: Gaussian bandreject filter
 $D_0 = 100, W = 6$

Bandpass Filter

Bandpass Filter (26)

The Bandpass filter performs the opposite of a bandreject filter and thus lets pass the frequencies in a narrow band of width W around D_0 . The transfer function $H(u, v)$ can be obtained from a corresponding bandreject filter by using the equation

$$H_{bp} = 1 - H_{br} \quad (6.18)$$

The perspective plots of the corresponding filters are depicted in Fig [6.20](#).

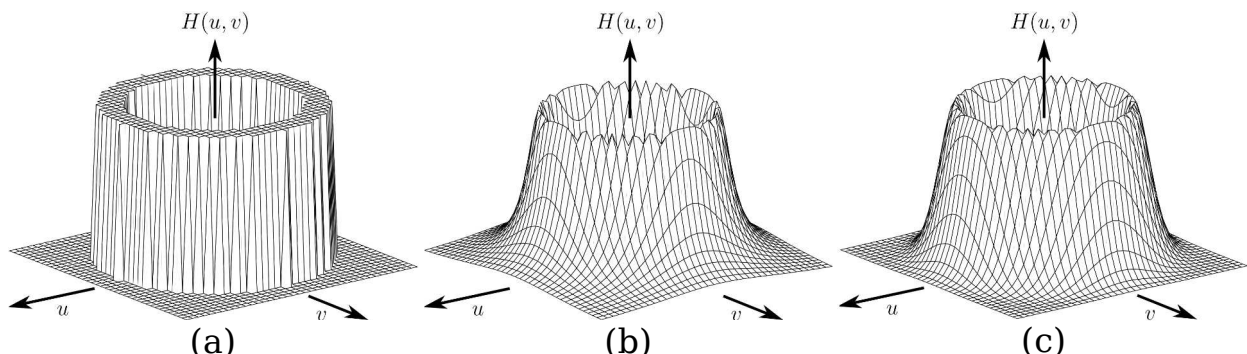


Fig 6.20 (a) Ideal bandpass filter, (b) Butterworth bandpass filter, and (c) Gaussian bandpass filter

Bandpass Filter Example (27)



Fig 6.21: Aerial image of Pompeii
with periodic noise

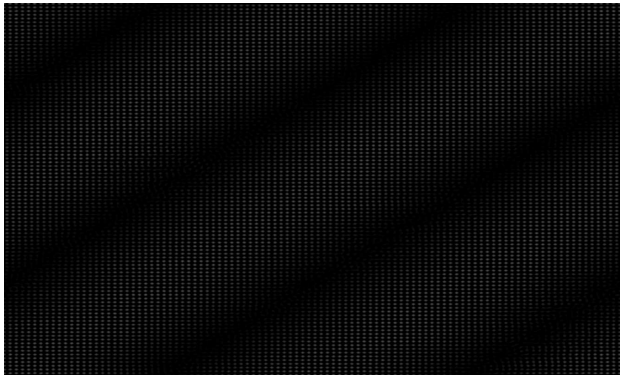


Fig 6.22: Ideal bandpass filter
 $D_0 = 100, W = 6$

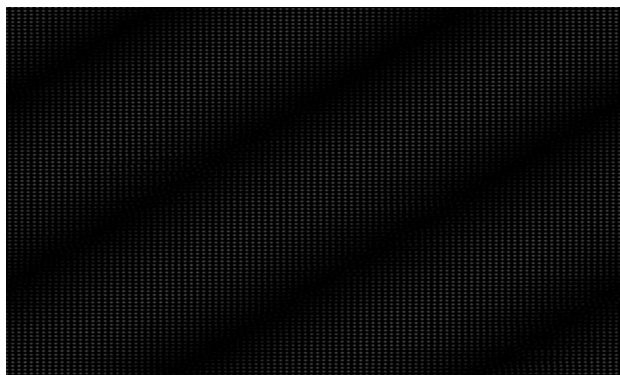


Fig 6.23: Butterworth bandpass
filter $D_0 = 100, W = 6$

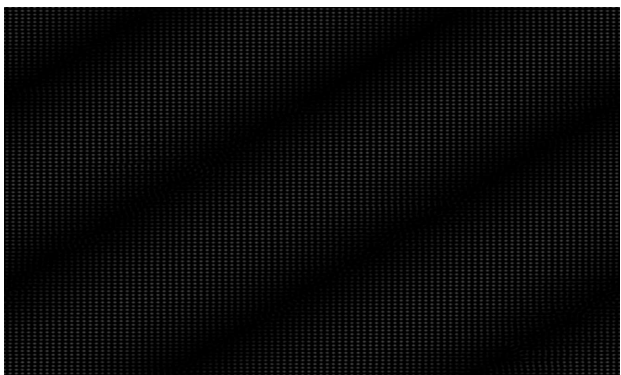


Fig 6.24: Gaussian bandpass filter
 $D_0 = 100, W = 6$

Notch Filter

Notch Filter (29)

A Notch filter *rejects* or *passes* frequencies in predefined neighbourhoods about a centre frequency. Due to the symmetry of the Fourier transform, notch filters must appear in symmetric pairs about the origin (except the one at the origin).

The transfer functions of the ideal, Butterworth, and Gaussian notch reject filter of radius (width) D_0 with centres at (u_0, v_0) and, by symmetry, at $(-u_0, -v_0)$, are

Ideal Notch Filter

$$H(u, v) = \begin{cases} 0 & \text{if } D_1(u, v) \leq D_0 \text{ or } D_2(u, v) \leq D_0 \\ 1 & \text{otherwise} \end{cases} \quad (6.19)$$

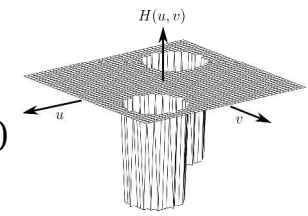


Fig 6.25: Ideal notch filter

Butterworth Notch Filter

$$H(u, v) = \frac{1}{1 + \left[\frac{D_0^2}{D_1(u, v)D_2(u, v)} \right]^n} \quad (6.20)$$

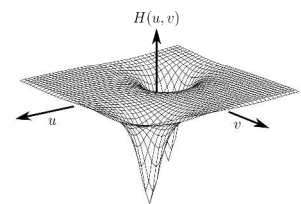


Fig 6.26: Butterworth notch filter

Gaussian Notch Filter

$$H(u, v) = 1 - e^{-\frac{1}{2} \left[\frac{D_1(u, v)D_2(u, v)}{D_0^2} \right]} \quad (6.21)$$

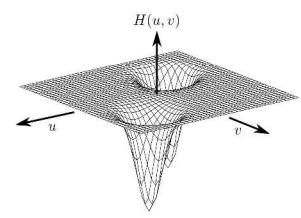


Fig 6.27: Gaussian notch filter

where

$$D_1(u, v) = [(u - M/2 - u_0)^2 + (v - N/2 - v_0)^2]^{\frac{1}{2}} \quad (6.22)$$

$$\underline{D_2(u, v)} = [(u - M/2 + u_0)^2 + (v - N/2 + v_0)^2]^{\frac{1}{2}}$$

Notch Filter (2) (30)

Similar to the bandpass/bandreject filters, the Notch reject filters can be turned into Notch pass filters with the relation

$$H_{np}(u, v) = 1 - H_{nr}(u, v) \quad (6.23)$$

where $H_{np}(u, v)$ is the transfer function of the notch pass filter, and $H_{nr}(u, v)$ the corresponding Notch reject filter.

If $u_0 = v_0 = 0$

- the *Notch reject filter* becomes a *highpass filter* and
- the *Notch pass filter* becomes a *lowpass filter*.

Ideal Notch Filter (31)

$D_0=16$ Example



Fig 6.28: Pompeii aerial image with periodic noise



Fig 6.29: Notch reject filtered image

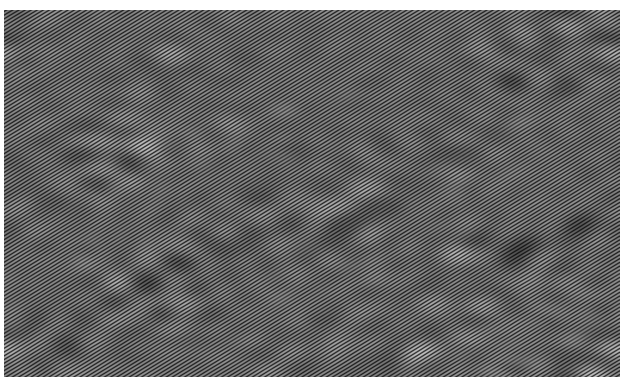


Fig 6.30: Notch pass filtered image (contrast enhanced)

Butterworth Notch Filter (32)

$D_0=64$ Example



Fig 6.31: Pompeii aerial image with periodic noise



Fig 6.32: Notch reject filtered image

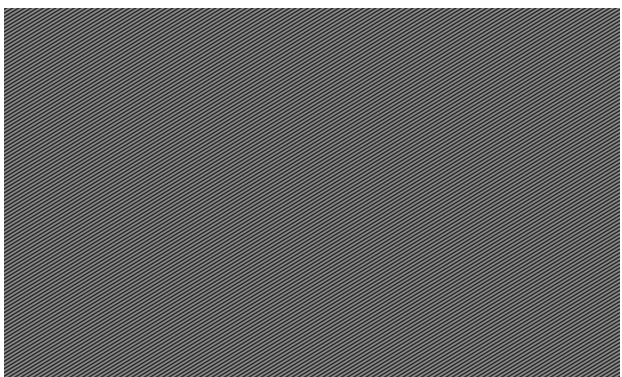


Fig 6.33: Notch pass filtered image (contrast enhanced)

Gaussian Notch Filter (33)

$D_0=64$ Example



Fig 6.34: Pompeii aerial image with periodic noise



Fig 6.35: Notch reject filtered image

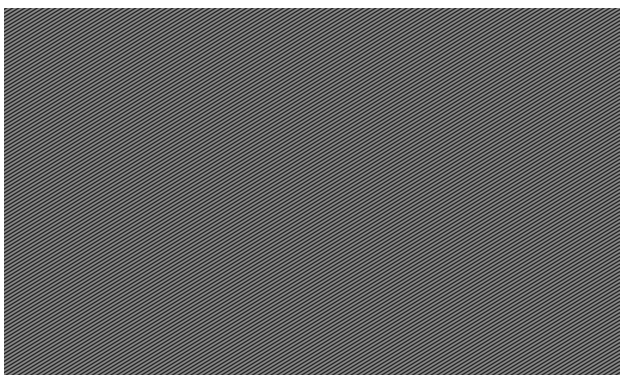


Fig 6.36: Notch pass filtered image (contrast enhanced)

General Notch Filter Example (34)



Fig 6.37: Original Mariner 6 martian image

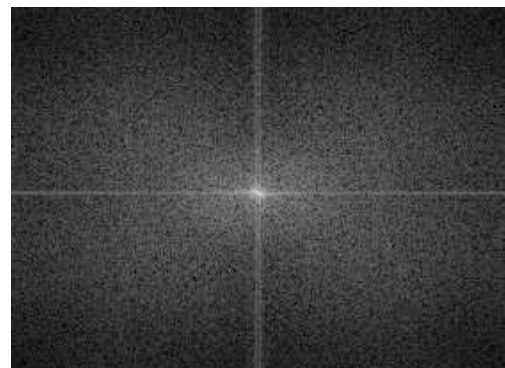


Fig 6.38: Log Fourier spectra of the image

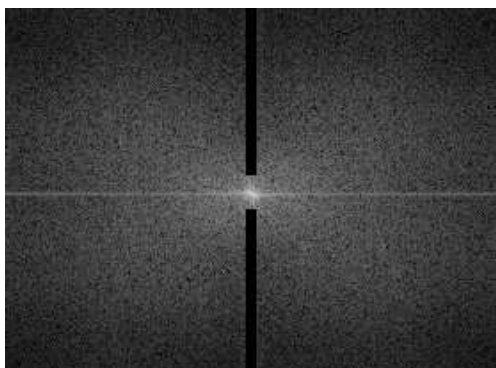


Fig 6.39: Notch filtered log spectra



Fig 6.40: Notch filtered image

Optimum Notch Filtering

Optimum Notch Filtering(36)

Images derived from electro-optical scanners, such as those used in space and aerial imaging, are sometimes corrupted by coupling and amplification of low-level signals in the scanners' circuitry. The resulting images tend to contain substantial periodic noise. The interference pattern are, however, in practice not always as clearly defined as in the samples shown thus far.

The first step in Optimum notch filtering is to *find* the *principal frequency* components and *placing notch pass filters* at the location of *each spike*, yielding $H(u, v)$. The Fourier transform of the interference pattern is thus given by

$$N(u, v) = H(u, v)G(u, v) \quad (6.24)$$

where $G(u, v)$ is the Fourier transform of the corrupted image. The corresponding interference pattern in the spatial domain is obtained with the inverse Fourier transform

$$\eta(x, y) = \mathcal{F}^{-1}\{H(u, v)G(u, v)\} \quad (6.25)$$

As the corrupted image $g(x, y)$ is assumed to be formed by the addition of the uncorrupted image $f(x, y)$ and the interference noise $\eta(x, y)$

$$g(x, y) = f(x, y) + \eta(x, y) \quad (6.26)$$

If the noise term $\eta(x, y)$ were known completely, subtracting it from $g(x, y)$ would yield $f(x, y)$. The problem is of course that the estimated interference pattern $\eta(x, y)$ is only an approximation. The effect of components not present in the estimate $\eta(x, y)$ can be minimised by subtracting from $g(x, y)$ a *weighted* portion of $\eta(x, y)$ to obtain an estimate for $f(x, y)$

$$\hat{f}(x, y) = g(x, y) - \omega(x, y)\eta(x, y) \quad (6.27)$$

where $\hat{f}(x, y)$ is the estimate of $f(x, y)$, and $\omega(x, y)$ is to be determined and optimises $\hat{f}(x, y)$ in some meaningful way.

One common approach is to select $\omega(x, y)$ so that the variance of $\hat{f}(x, y)$ is minimised over a specified neighbourhood of size $(2a + 1) \times (2b + 1)$ about every point (x, y) .

$$\sigma^2(x, y) = \frac{1}{(2a+1)(2b+1)} \sum_{s=-a}^a \sum_{t=-b}^b [\hat{f}(x+s, y+t) - \bar{\hat{f}}(x, y)]^2 \quad (6.29)$$

where $\bar{\hat{f}}(x, y)$ is the average value of $\hat{f}(x, y)$ in the neighbourhood; that is

$$\bar{\hat{f}}(x, y) = \frac{1}{(2a+1)(2b+1)} \sum_{s=-a}^a \sum_{t=-b}^b \hat{f}(x+s, y+t) \quad (6.30)$$

Substituting Eq 6.27 into Eq 6.29 yields

$$\begin{aligned} \sigma^2(x, y) &= \frac{1}{(2a+1)(2b+1)} \sum_{s=-a}^a \sum_{t=-b}^b ([g(x+s, y+t) \\ &\quad - \omega(x+s, y+t)\eta(x+s, y+t)] \\ &\quad - [\bar{g}(x, y) - \bar{\omega}(x, y)\eta(x, y)])^2 \end{aligned} \quad (6.31)$$

Assuming that $\omega(x, y)$ remains constant over the neighbourhood gives the approximation

$$\omega(x+s, y+t) = \omega(x, y) \quad (6.32)$$

for $-a \leq s \leq a$ and $-b \leq t \leq b$. This assumption results in the expression

in the neighbourhood. With these approximations Eq 6.30 becomes

$$\begin{aligned}\sigma^2(x, y) &= \frac{1}{(2a+1)(2b+1)} \sum_{s=-a}^a \sum_{t=-b}^b ([g(x+s, y+t) \\ &\quad - \omega(x, y)\eta(x+s, y+t)] - [\bar{g}(x, y) - \omega(x, y)\bar{\eta}(x, y)])^2\end{aligned}\quad (6.34)$$

To minimise $\sigma^2(x, y)$, we solve

$$\frac{\partial \sigma^2(x, y)}{\partial \omega(x, y)} = 0 \quad (6.35)$$

for $\omega(x, y)$. The result is

$$\omega(x, y) = \frac{\overline{g(x, y)\eta(x, y)} - \bar{g}(x, y)\bar{\eta}(x, y)}{\overline{\eta^2}(x, y) - \bar{\eta}^2(x, y)} \quad (6.36)$$

To obtain an estimated restored image $\hat{f}(x, y)$, $\omega(x, y)$ must be computed from Eq 6.36 and substituted into Eq 6.27 to determine $\hat{f}(x, y)$.

Optimum Notch Filtering(37) Principle

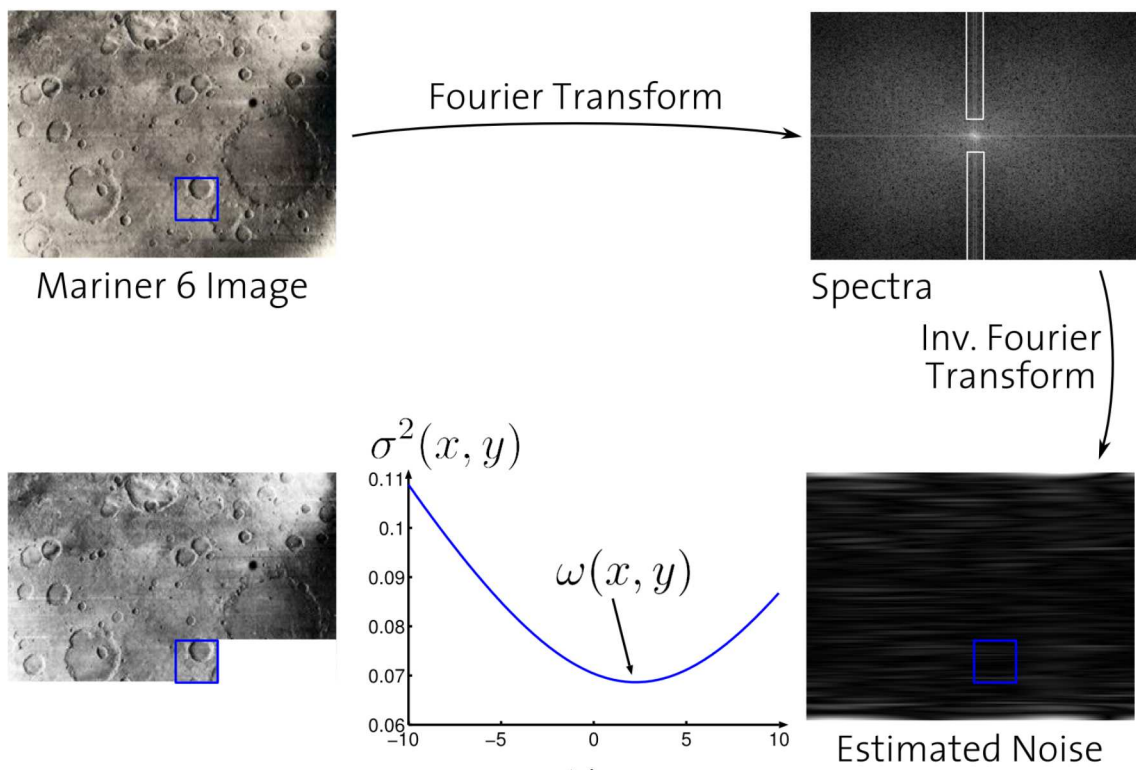


Fig 6.41 Principle of the optimum notch filter

Optimum Notch Filter (38) Example



Fig 6.42 Aerial image of Pompeii with heavy periodic noise distortions



Fig 6.43 Noise estimation with Gaussian notch pass filter



Fig 6.44 Notch reject filtered image



Fig 6.45 Result filtered with an optimum notch filter of size 20×20

Optimum Notch Filter (39)

Example with Pixel Increments



Fig 6.46 Aerial image of Pompeii corrected with the optimal notch filter of size 50×50 with the window shifted pixelwise

Optimum Notch Filter (40)

Example with Pixel Increments (2)

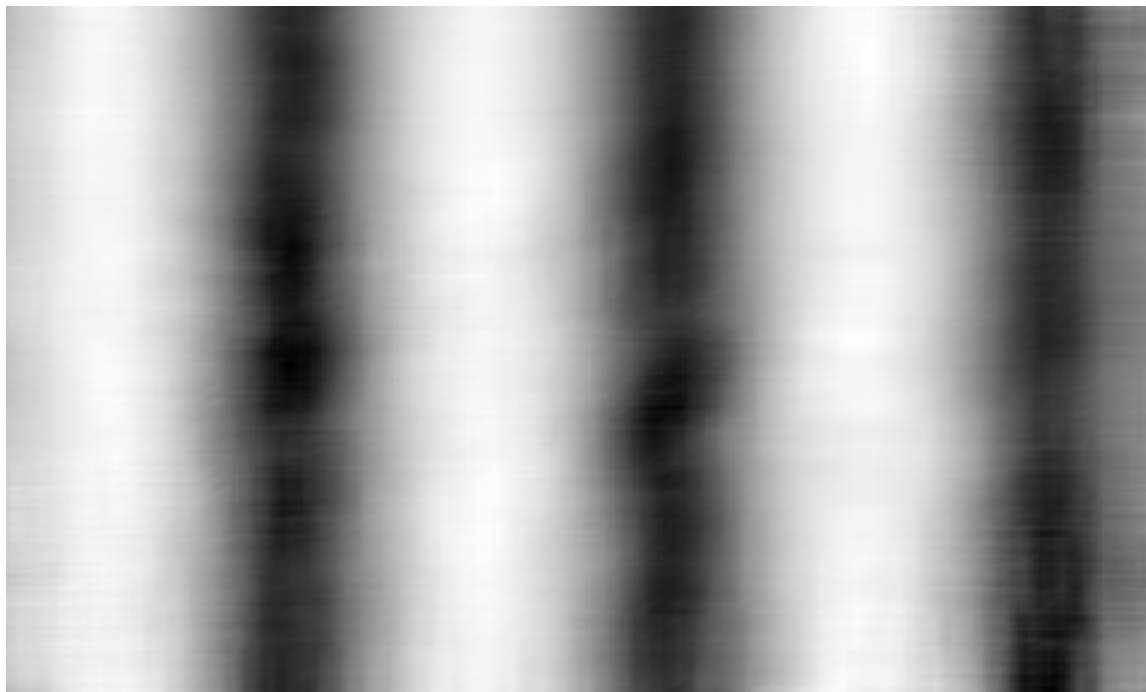
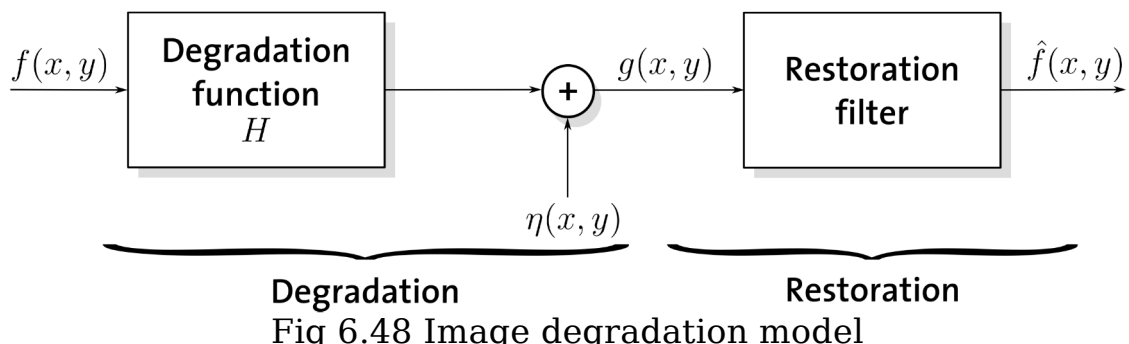


Fig 6.47 $\omega(x, y)$ of the example image in Fig [6.46](#)

Estimating the Degradation Function

Estimating the Degradation Function (42)

So far we concentrated mainly at the additive noise term $\eta(x, y)$. In the remainder of this presentation we concentrate on ways to remove the degradation function H .



Estimating the Degradation Function (2) (43)

There are three principle methods to estimate the degradation function H

1. Observation
2. Experimentation
3. Mathematical modelling

The process of restoring a corrupted image using the estimated degradation function is sometimes called blind deconvolution, as the true degradation is seldom known completely.

In recent years a forth method based on maximum-likelihood estimation (MLE) often called blind deconvolution has been proposed.

Beware: All multiplications/divisions in the equations in this part of the lecture are componentwise.

Estimating by Image Observation (44)

Given

A degraded image without any information about the degradation function H .

Solution

1. Select a subimage with strong signal content $\rightarrow g_s(x, y)$
2. By estimating the sample grey levels of the object and background in $g_s(x, y)$ we can construct an unblurred image of the same size and characteristics as the observed subimage $\rightarrow \hat{f}_s(x, y)$
3. Assuming that the effect of noise is negligible (thus the choice of a strong signal area), it follows from Eq [6.2](#) that

$$H_s(u, v) = \frac{G_s(u, v)}{\hat{F}_s(u, v)}$$

4. Thanks to the *shift invariance* we can deduce $H(u, v)$ from $H_s(u, v)$

Estimating by Experimentation (45)

Given

Equipment similar to the equipment used to acquire the degraded image

Solution

1. Images similar to the degraded image can be acquired with various system settings until it closely matches the degraded image
2. The system can then be characterised by measuring the impulse (small bright dot of light) response. A linear, shift invariant system can be fully described by its impulse response.
3. As the Fourier transform of an impulse is a constant, it follows from Eq [6.2](#)

$$H(u, v) = \frac{G(u, v)}{A}$$

where $G(u, v)$ is the Fourier transform of the observed image, and A is a constant describing the strength of the impulse.

Estimating by Mathematical Modelling (46)

Degradation modelling has been used for many years. It, however, requires an indepth understanding of the involved physical phenomenon. In some cases it can even incorporate environmental conditions that cause degradations. Hufnagel and Stanly proposed in 1964 a model to characterise atmospheric turbulence.

$$H(u, v) = e^{-k(u^2 + v^2)^{5/6}} \quad (6.37)$$

where k is a constant that depends on the nature of the turbulence.

Except of the 5/6 power the above equation has the same form as a Gaussian lowpass filter.

Illustration of the Atmospheric Turbulence Model (47)



Fig 6.49: Aerial image of Pompeii



Fig 6.50: Pompeii with mild turbulence $k = 0.00025$



Fig 6.51: Pompeii with medium turbulence $k = 0.001$



Fig 6.52 Pompeii with heavy turbulence $k = 0.0025$

Inverse Filtering

Direct Inverse Filtering

Direct Inverse Filtering (50)

The simplest approach to restore a degraded image is to form an estimate of the form

$$\hat{F}(u, v) = \frac{G(u, v)}{H(u, v)} \quad (6.38)$$

and then obtain the corresponding image by inverse Fourier transform. This method is called direct inverse filtering. With the degradation model Equation [6.2](#) we get

$$\hat{F}(u, v) = F(u, v) + \frac{N(u, v)}{H(u, v)} \quad (6.39)$$

This simple equation tells us that, *even if we knew $H(u, v)$ exactly we could not recover the undegraded image $f(x, y)$ completely* because:

1. the noise component is a random function whose Fourier transform $N(u, v)$ is not known, and
2. in practice $H(u, v)$ can contain numerous zeros.

Direct Inverse filtering is seldom a suitable approach in practical applications

Two Practical Approaches for Inverse Filtering (51)

1. Low Pass Filter

$$\hat{F}(u, v) = \frac{G(u, v)}{H(u, v)} L(u, v) \quad (6.40)$$

where $L(u, v)$ is a low-pass filter that should eliminate the very low (or even zero) values often experienced in the high frequencies.

2. Constrained Division

$$\hat{F}(u, v) = \begin{cases} \frac{G(u, v)}{H(u, v)} & \text{if } |H(u, v)| \geq d \\ G(u, v) & \text{if } |H(u, v)| < d \end{cases} \quad (6.41)$$

gives values, where $H(u, v)$ is lower than a threshold d a special treatment.

These approaches are also known as Pseudo-Inverse Filtering.

Artificial Inverse Filtering Example (52)

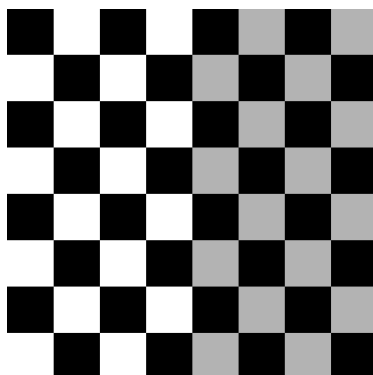


Fig 6.53: Checkerboard sample

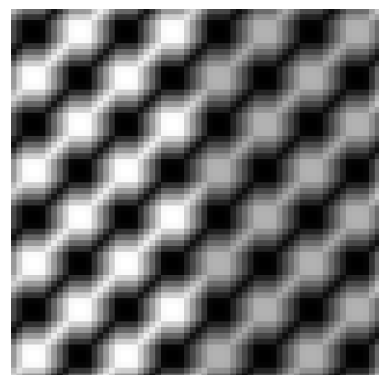


Fig 6.54: Motion blur of 7 pixel in 45° direction

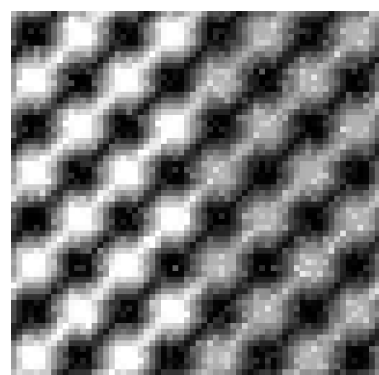
Fig 6.55: Additive noise with $\mu = 0, \sigma = 0.1$ 

Fig 6.56: Motion and noise degraded checkerboard

Artificial Inverse Filtering Example (2) (53)

Although very tempting from its simplicity, the *direct inverse filtering* approach does not work for practical applications. Even if the degradation H is known exactly.

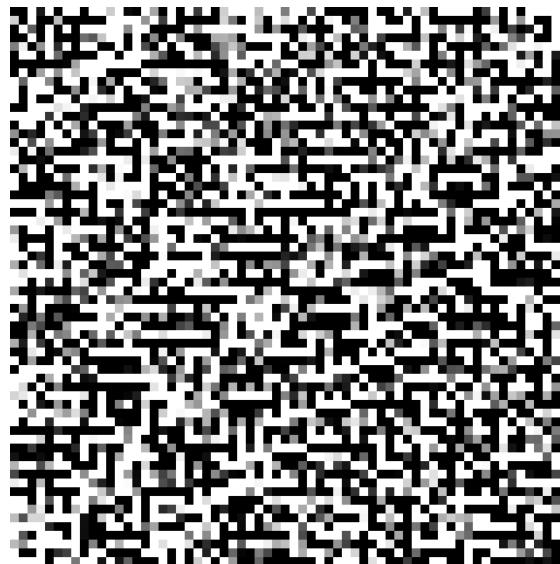


Fig 6.57: Direct inverse filtering result

Inverse Filtering Example (2) (54)



Fig 6.58: Inverse filtering of Figure [6.52](#)



Fig 6.59: Pseudo Inverse filtering for freq. radius ≤ 40



Fig 6.60: Pseudo Inverse filtering for frequencies radius ≤ 80

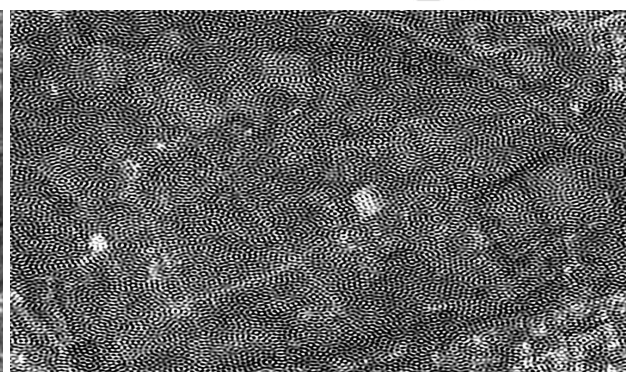


Fig 6.61: Pseudo Inverse filtering for frequencies radius ≤ 120

Wiener Filtering

Wiener Filtering (56)

The best known improvement to *inverse filtering* is the Wiener Filter. The Wiener filter seeks an estimate \hat{f} that minimises the statistical error function

$$e^2 = E\{(f - \hat{f})^2\} \quad (6.42)$$

where E is the expected value and f the undegraded image. The solution to this equation in the frequency domain is

$$\hat{F}(u, v) = \left[\frac{1}{H(u, v)} \frac{|H(u, v)|^2}{|H(u, v)|^2 + S_\eta(u, v)/S_f(u, v)} \right] G(u, v) \quad (6.43)$$

where

- $H(u, v)$ is the degradation function
- $|H(u, v)|^2 = H^*(u, v)H(u, v)$ with $H^*(u, v)$ the complex conjugate of H
- $S_\eta(u, v) = |N(u, v)|^2$ is the power spectrum of the noise
- $S_f(u, v) = |F(u, v)|^2$ is the power spectrum of the undegraded image

Wiener Filtering (2) (57)

If the *noise spectrum* $|N(u, v)|^2$ is zero, the *noise-to-signal power ratio* $S_\eta(u, v)/S_f(u, v) = |N(u, v)|^2/|F(u, v)|^2 = 0$ vanishes and the *Wiener Filter* reduces to the *inverse filter*.

$$\begin{aligned}
 \hat{F}(u, v) &= \left[\frac{1}{H(u, v)} \frac{|H(u, v)|^2}{|H(u, v)|^2 + \textcolor{red}{S}_\eta(\textcolor{red}{u}, \textcolor{red}{v})/S_f(u, v)} \right] G(u, v) \\
 &= \left[\frac{1}{H(u, v)} \frac{|H(u, v)|^2}{|H(u, v)|^2 + 0} \right] G(u, v) \\
 &= \frac{1}{H(u, v)} G(u, v)
 \end{aligned} \tag{6.44}$$

This is no problem, as the *inverse filter* works fine if no noise is present.

Parametric Wiener Filter (58)

The *main problem* with the *Wiener filter* is that the *power spectrum* $|F(u, v)|^2$ of the *undegraded image* is *seldom known*.

A frequently used approach when these quantities cannot be estimated is to approximate Eq 6.43 by the expression

$$\hat{F}(u, v) = \left[\frac{1}{H(u, v)} \frac{|H(u, v)|^2}{|H(u, v)|^2 + K} \right] G(u, v) \quad (6.45)$$

where K is a user selected constant.

This simplification can be partly justified when dealing with spectrally white noise, where the noise spectrum $S_\eta(u, v) = |N(u, v)|^2$ is constant. However, the problem still remains that the power spectrum $S_f(u, v) = |F(u, v)|^2$ of the undegraded image is unknown and must be estimated.

Even if the actual ratio K is not known, it becomes a simple matter to experiment interactively varying the constant and viewing the results.

Artificial Wiener Filtering Example (59)

This example shows the performance of the Wiener filter on the example Fig 6.56 using (1) the approximation of Eq 6.45 with $K = 0.04$ in Fig 6.62 and (2) the Wiener filter using full knowledge of the noise and undegraded image's power spectra in Fig 6.63.

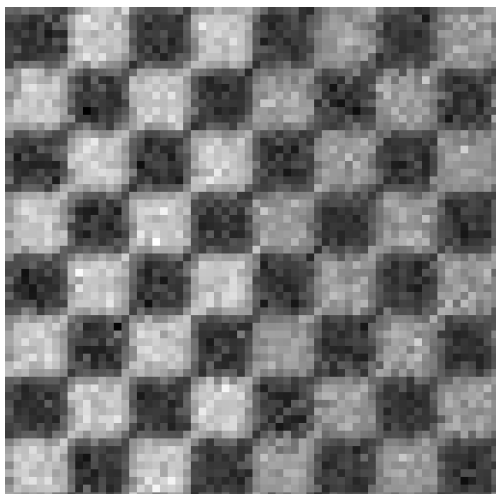


Fig 6.62: Parametric Wiener filter using a constant ratio

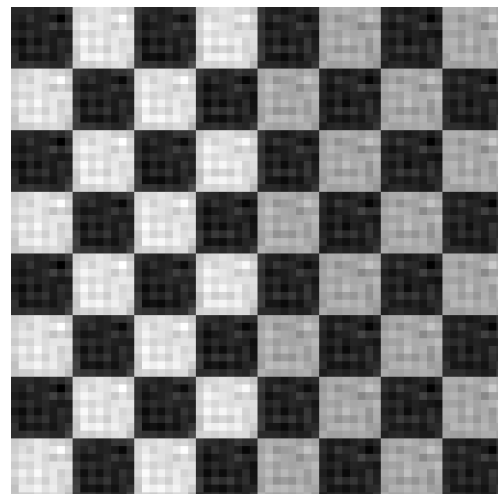


Fig 6.63: Wiener filter knowing the noise and undegraded signal power spectra

Wiener Filtering (60)

Example with Little Noise

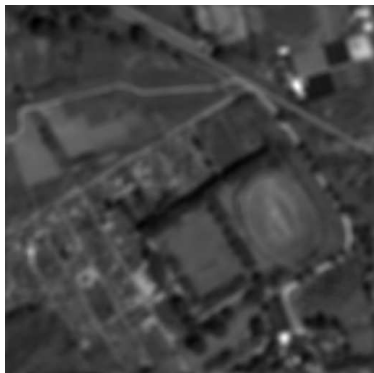


Fig 6.64: Pompeii blurred with Gaussian kernel $\sigma = 5$, and Gaussian noise $\mu = 0, \sigma = 0.001$



Fig 6.65: Result of direct inverse filtering



Fig 6.66: Result with Parametric Wiener filtering $K = 0.0001$



Fig 6.67: Result with Wiener filtering

Wiener Filtering (61) Example with Medium Noise



Fig 6.68: Pompeii blurred with Gaussian kernel $\sigma = 5$, and Gaussian noise $\mu = 0, \sigma = 0.01$



Fig 6.69: Result of direct inverse filtering



Fig 6.70: Result with Parametric Wiener filtering $K = 0.0001$



Fig 6.71: Result with Wiener filtering

Wiener Filtering (62)

Example with Heavy Noise



Fig 6.72: Pompeii blurred with Gaussian kernel $\sigma = 5$, and Gaussian noise $\mu = 0, \sigma = 0.1$



Fig 6.73: Result of direct inverse filtering



Fig 6.74: Result with Parametric Wiener filtering $K = 0.0001$



Fig 6.75: Result with Wiener filtering

Comparison Param. (63) Wiener vs. Wiener Filtering

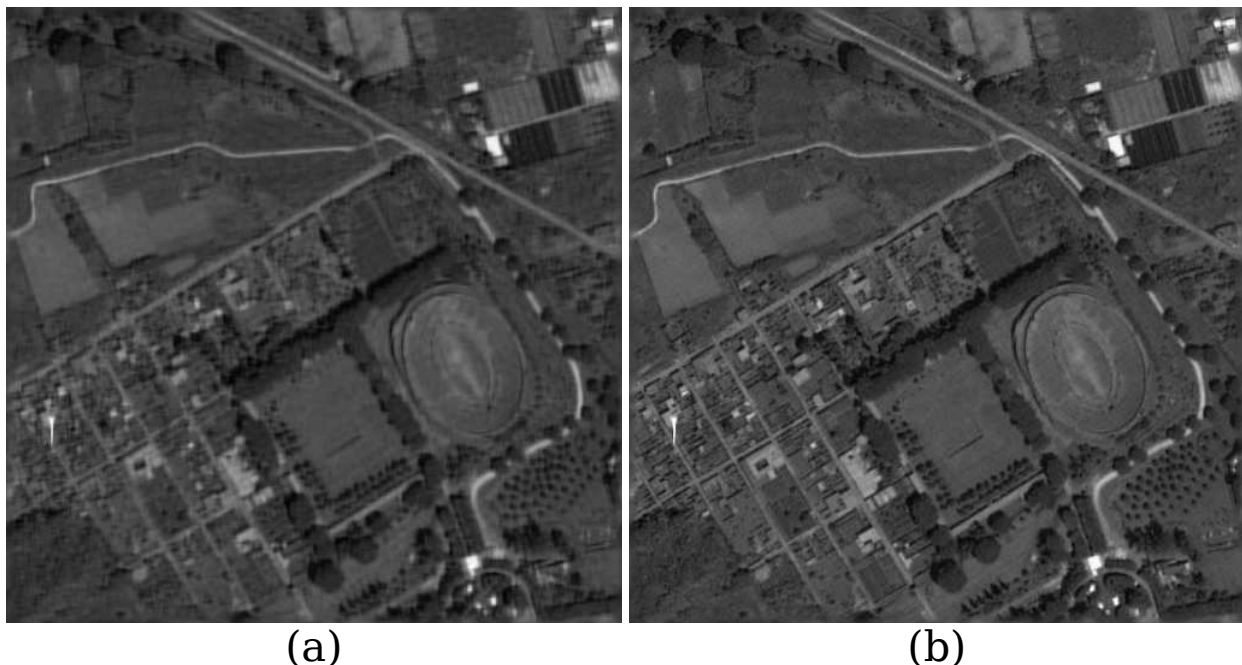


Fig 6.76 Aerial image of Pompeii with Gaussian blur ($\sigma = 5$) and noise ($\mu = 0, \sigma = 0.1$) (a) restored with the Parametric Wiener ($K = 0.0001$), (b) same image restored with Wiener filter.

Drawback of the Wiener (64) Filter

The problem of having to know something about the degradation function $H(u, v)$ is common to all methods discussed in this part.

The *Wiener filter* has the additional difficulty, that

- the power spectra of the undegraded image and
- the power spectra of the noise

must be known.

Although an approximation by a constant is possible as in the *Parametric Wiener filter*, see Fig 6.62, this approach is not always suitable.

Geometric Mean Filter

Geometric Mean Filter (66)

The Geometric Mean Filter is a generalisation of *inverse filtering* and the *Wiener filtering*. Through its parameters α, β it allows access to an entire family of filters.

$$\hat{F}(u, v) = \left[\frac{H^*(u, v)}{|H(u, v)|^2} \right]^\alpha \left[\frac{H^*(u, v)}{|H(u, v)|^2 + \beta \frac{S_\eta(u, v)}{S_f(u, v)}} \right]^{1-\alpha} G(u, v) \quad (6.46)$$

Depending on the parameters α, β the filter characteristics can be adjusted

- $\alpha = 1$: inverse filtering
- $\alpha = 1/2, \beta = 1$: spectrum equalisation filter
- $\alpha = 0$: parametric Wiener filter $\rightarrow \beta = 1$ Wiener

Constrained Least Squares Filtering

Constrained Least Squares (Regularised) Filtering (68)

The Constrained Least Squares Filtering approach only requires knowledge of the mean and variance of the noise. As shown in previous lectures these parameters can be usually estimated from the degraded image.

The definition of the 2D discrete convolution is

$$h(x, y) * f(x, y) = \frac{1}{MN} \sum_{m=0}^{M-1} \sum_{n=0}^{N-1} f(m, n)h(x - m, y - n) \quad (6.47)$$

Using this equation we can express the linear degradation model $g(x, y) = h(x, y) * f(x, y) + \eta(x, y)$ in vector notation as

$$\mathbf{g} = \mathbf{H}\mathbf{f} + \boldsymbol{\eta} \quad (6.48)$$

Constrained Least Squares Filtering (2)

It seems obvious that the restoration problem is now reduced to simple matrix manipulations. Unfortunately this is not the case. The problem with the matrix formulation is that the *H* matrix is very large $MN \times MN$ and that its *inverse* is firstly very sensitive to noise and secondly does not necessarily exist.

One way to deal with these issues is to *base optimality* of restoration on a *measure of smoothness*, such as the second derivative of the image, e.g. the *Laplacian*.

$$C = \sum_{x=0}^{M-1} \sum_{y=0}^{N-1} [\nabla^2 f(x, y)] \quad (6.49)$$

subject to the constraint

$$\|\mathbf{g} - \mathbf{H}\hat{\mathbf{f}}\|^2 = \|\eta^2\| \quad (6.50)$$

where $\|\cdot\|$ is the Euclidian norm, and \hat{f} an estimate of the undegraded image.

Constrained Least Squares Filtering (3) (70)

The *Frequency domain solution* to this optimisation problem is given by

$$\hat{F}(u, v) = \left[\frac{H^*(u, v)}{|H(u, v)|^2 + \gamma|P(u, v)|^2} \right] G(u, v) \quad (6.51)$$

where γ is a parameter that must be adjusted so that the constraint in Eq 6.50 is satisfied, and $P(u, v)$ is the Fourier transform of the Laplace operator

$$p(x, y) = \begin{bmatrix} 0 & -1 & 0 \\ -1 & 4 & -1 \\ 0 & -1 & 0 \end{bmatrix} \quad (6.52)$$

Note: $p(x, y)$ must be properly padded with zeros prior to computing the Fourier transform.

It is possible to adjust the parameter γ interactively until acceptable results are obtained.

Optimal Selection for Gamma (71)

If we are interested in optimality, the parameter γ must be adjusted so that the constraint $\|\mathbf{g} - \mathbf{H}\hat{\mathbf{f}}\|^2 = \|\eta^2\|$ in Eq [6.50](#) is satisfied.

It turns out that

$$\gamma = MN[\sigma_\eta^2 + m_\eta^2] \quad (6.53)$$

is the optimal selection given the above optimisation equation where σ_η, m_η are the mean and variance of the noise.

It is important to understand, that optimum restoration in the sense of *constrained least squares* does not necessarily imply *best* in the visual sense. In general, automatic determined restoration filters yield inferior results to manual adjustment of filter parameters.

Artificial Constrained Least Squares Filter Example (72)

This example shows the performance of the Constrained Least Squares Filter on the example Fig 6.56 using (1) the theoretical optimal value for $\gamma = 40.96$ in Fig 6.77 and (2) the constrained least squares filter with a manually selected γ of 10.1861 6.78.

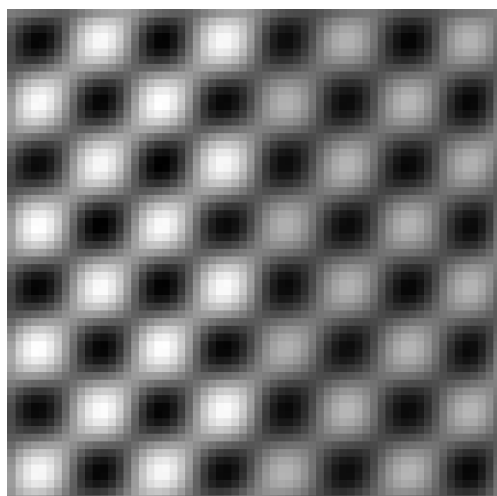


Fig 6.77: Result with optimal γ

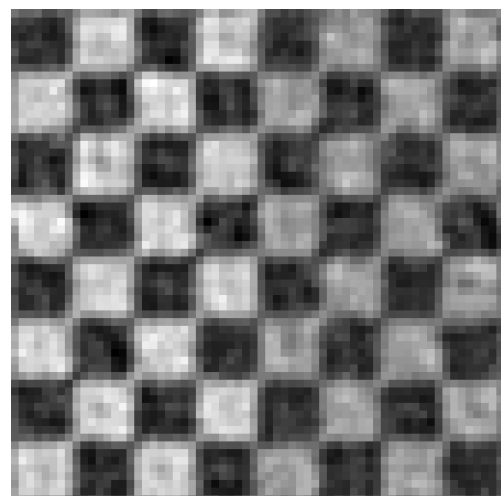


Fig 6.78: Results with manually selected γ

Constrained Least Squares Filter Example (73)



Fig 6.79: Pompeii blurred with Gaussian kernel $\sigma = 5$



Fig 6.80: Result with low Gaussian noise of $\sigma = 0.001$



Fig 6.81: Result with medium Gaussian noise of $\sigma = 0.01$



Fig 6.82: Result with high Gaussian noise of $\sigma = 0.1$